Passive Q-Switching of an All-Fiber Laser Using WS$_2$-Deposited Optical Fiber Taper
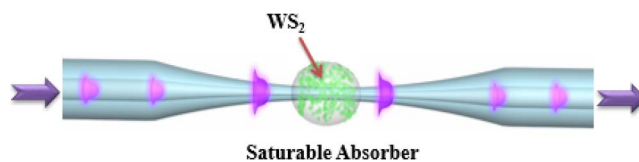
Reza Khazaeinezhad
Tavakol Nazari
Hwanseong Jeong
Kyung Jun Park
Byoung Yoon Kim, Member, IEEE
Dong-Il Yeom
Kyunghwan Oh, Member, IEEE

Passive Q-Switching of an All-Fiber Laser Using WS₂-Deposited Optical Fiber Taper

Reza Khazaeinezhad,[1] Tavakol Nazari,[1] Hwanseong Jeong,[2]
Kyung Jun Park,[3] Byoung Yoon Kim,[3] *Member, IEEE*,
Dong-Il Yeom,[2] and Kyunghwan Oh,[1] *Member, IEEE*

[1]Photonic Device Physics Laboratory, Institute of Physics and Applied Physics, Yonsei University, Seoul 120-749, Korea
[2]Department of Physics and Energy Systems Research, Ajou University, Suwon 443-749, Korea
[3]Department of Physics, Korea Advanced Institute of Science and Technology, Daejeon 305-701, Korea

Abstract: We demonstrate the passive Q-switching operation of an erbium-doped fiber laser using a few-layer WS₂-based saturable absorber with evanescent field interaction. WS₂ flakes have been synthesized via a liquid-phase exfoliation method, and an optical fiber taper was selected as a light-material template that causes to achieve a long interaction length of the evanescent wave. Subsequently, the prepared solution was optically deposited around the 3-mm interaction length of the fabricated optical fiber taper with a 5-μm waist diameter. The proposed Q-switched fiber laser based on the WS₂-deposited fiber taper saturable absorber could generate stable output pulses at 1565 nm, with a pulsewidth ranging from 1.3 to 3 μs and a repetition rate of 33–108 kHz.

Index Terms: Tungsten disulfide, nonlinear optical materials, saturable absorber, Q-switched fiber laser.

1. Introduction

Q-switched fiber lasers have attracted great attention owing to the relatively large pulse energy at relatively low repetition rates and pulse width of the scale from microsecond to nanosecond. These short pulsed lasers have extensive applications in material processing, telecommunications, medicine, and sensing [1]. Q-switched pulses can be obtained via active or passive Q-switching techniques. Passively Q-switched lasers have several advantages such as simplicity, compactness, and low cost compared to that of active techniques which require an active optical component such as electro-optic or acousto-optic modulators [2].

Passive Q-switched technique of lasers based on saturable absorber (SA) is the well-known and most effective method to achieve Q-switching operation which has been widely investigated. In the past few decades, researchers investigated various kinds of SA materials, including toxic dye materials [3], semiconductor saturable absorber mirrors (SESAMs) [4], carbon nanotubes (CNTs) [5], and graphene [6], [7]. Although the SESAMs are very mature and commercialized,

they are still limited due to the complex and expensive fabrications, as well as having a narrow-band wavelength operation range [8]. The most cost-effective method was using carbon materials such as the carbon nanotubes where their working wavelengths were connected with the diameter of the nanotubes [9], as well as graphene with zero band-gap and small absorption [6].

Recently, transition metal dichalcogenides (TMDs) materials like molybdenum disulfide (MoS$_2$) and Tungsten disulfide (WS$_2$) attracted great attention due to the high saturable absorption of these materials [10]. TMDs are two-dimensional materials which their band-gap depends on the thickness. Their monolayers have a direct band-gap and as the number of layers increase the band-gap shifts toward indirect band-gap structure [11]. Due to their unique characteristics, they have been deeply studied in several research fields [12]. Moreover, TMDs have been used as the SA for mode locking and Q-switching technology in different structures [13]–[19].

Although the fiber ferrule type SA has been widely used due to the easy implementation, the mechanical contact is induced physical damage as well as causes to break all-fiber ring cavity configuration [20]. Due to the direct interaction of light with materials, this type of SA also decreases the damage threshold under high power regimes, especially in the presence of polymer binders. The saturable absorbers based on evanescent field interaction not only increase the damage threshold as well as light-material interaction length, but also maintain the all-fiber cavity structure. There are two practical templates for evanescent coupling structure including side-polished fiber and fiber taper [14], [19]. Side-polished fiber suffers of several drawbacks such as a complicated fabrication process and difficulty in making a fine polished surface, as well as high unavoidable polarization sensitivity due to the asymmetric structure [21]. So, we could assume that the fiber taper is one the best option for a light-material template in fiber laser configurations [18], [19]. So far, the application of WS$_2$ as a Q-switcher in an all fiber laser structure based on fiber taper saturable absorber has not been attempt yet, which will have a great impact in this field of study due to the simple and trustable fabrication process and compact proposing structure.

In this work, we propose and demonstrate an all-fiber passively Q-switched Erbium-doped fiber laser using the interaction of WS$_2$ flakes and the fiber taper's evanescent fields. WS$_2$-deposited fiber taper is demonstrated as a Q-switcher, for the first time to the best of our knowledge, to overcome the drawbacks of the sandwich structure and the side-polished ones. The few-layer WS$_2$ flakes are fabricated via liquid phase exfoliation method and optically deposited around the 5 μm waist diameter of the fabricated fiber taper. Subsequently, in order to confirm the saturable absorption characteristic, passively Q-switched pulses were obtained based on WS$_2$ SA in an all-fiber laser configuration with high thermal damage threshold and stability.

2. WS$_2$ Flakes Preparation and Saturable Absorber Fabrication

The fiber taper as a template for light material interaction is fabricated via the standard flame brushing technique [22]. The fiber taper was fabricated by fixing a single-mode fiber (SMF) at both ends in two fiber clamps and when the central region was heated, the fiber was stretched simultaneously at both sides. The insertion loss of the prepared tapered fiber was around 1 dB and the waist diameter and the interaction length of fiber taper are about 5 μm and 3 mm respectively, as shown in Fig. 1(a).

Then, we prepared a uniform solution to take full advantage of the optical properties of the 2D materials. The few layer WS$_2$ flakes were synthesized by well-known liquid phase exfoliation method (LPE) [23], as shown schematically in Fig. 1(b). LPE method involves three steps as follows: 1. Dispersion of bulk WS$_2$ in solvent; 2. Exfoliation process via ultra-sonication; 3. Using ultra-centrifuge to separate exfoliated few-layer WS$_2$ flakes from un-exfoliated thick flakes. The inset of Fig. 1(c). shows a picture of prepared uniform solution of WS$_2$ flakes in ethanol and Fig. 1(c). illustrates the SEM image of drop-casted WS$_2$ flakes on a SiO$_2$ substrate. Linear transmission of the prepared solution is depicted in Fig. 1(d). indicating the absorption peak of WS$_2$ at 625 nm and the inset shows transmission electron microscopy (TEM) images of the WS$_2$ flakes on a TEM substrate which confirms the very thin exfoliated flakes. Finally, as shown in
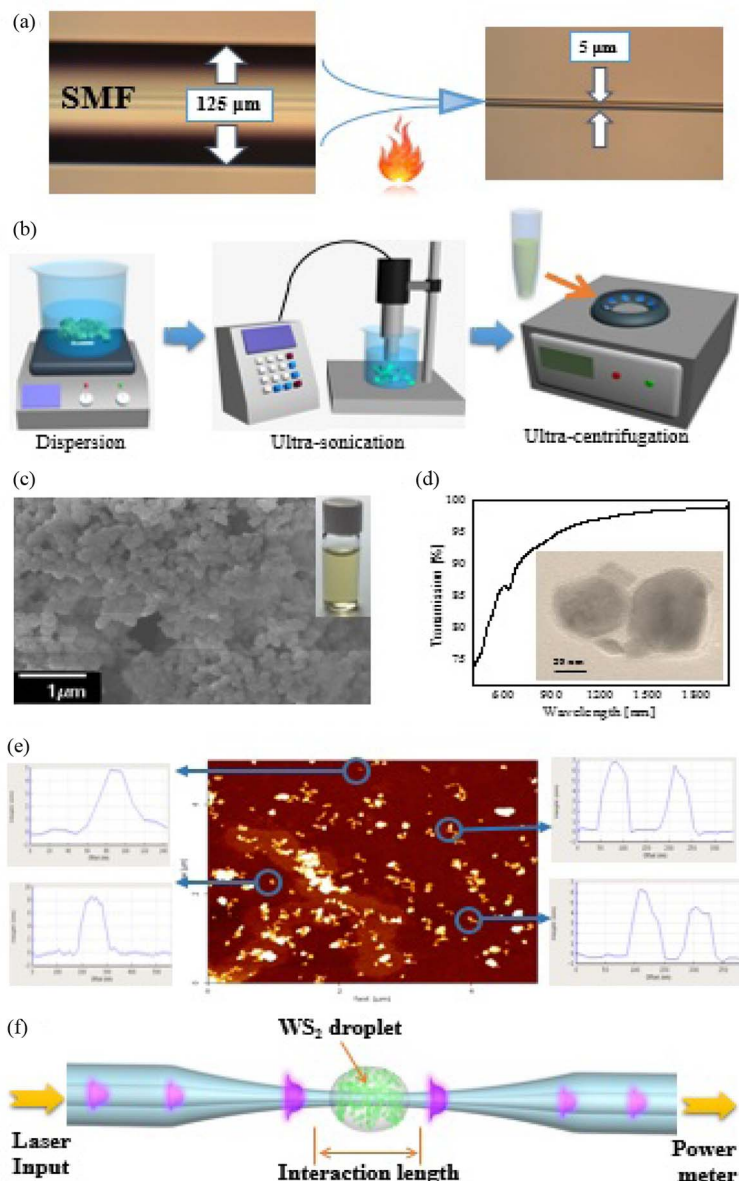
Fig. 1. (a) Tapering of a single mode fiber from 125 μm to 5 μm diameter via flame brushing method. (b) Liquid Phase Exfoliation process including 3 steps: first dispersion of bulk WS_2 in solvent, then exfoliation process using ultra-sonication, and finally ultra-centrifugation. (c) SEM image of the uniform size of the exfoliated few layer WS_2 flakes (inset: bottle of a well-dispersed WS_2 flakes in ethanol). (d) Transmittance of the WS_2 flakes via spectrophotometer (inset: TEM image of the exfoliated few layer WS_2 flakes). (e) AFM measurement results of the prepared flakes. (f) Optical deposition of WS_2 flakes onto the fiber taper via evanescent field interaction.

Fig. 1(e), the thickness of WS_2 flakes were measured via an atomic force microscopy (AFM), showing the thickness of 5 ~ 7 nm which corresponds to 8 ~ 10 layers [24].

Finally, we deposited the WS_2 onto the waist diameter of fabricated fiber taper to prepare saturable absorber as a Q-switcher. The evanescent light deposition of WS_2 flakes onto the fiber taper is schematically demonstrated in Fig. 1(f). The uniform solution is softly and slowly dripped onto the interaction length of the fiber taper while the 1.5 μm laser light pass through the fiber for optical deposition via the evanescent field. We monitored the transmission of the fiber taper during the deposition process by an optical power meter in order to control the deposition
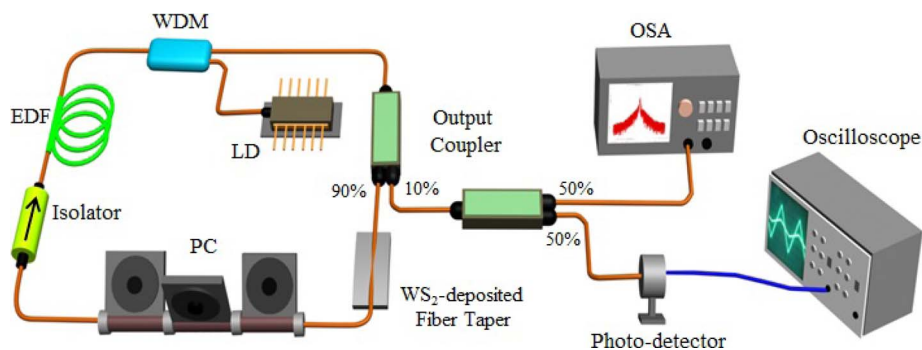
Fig. 2. Schematic diagram of passively Q-switched Er-doped fiber laser (LD: Laser Diode; WDM: Wavelength Division Multiplexer; EDF: Erbium-Doped Fiber; PC: Polarization Controller; OSA: Optical Spectrum Analyzer).

process. Since the waist diameter of the fiber taper is decreased to 5 μm, the propagating light will form the evanescent field in the air and consequently interact with the droplet of solution around the waist. After the deposition of WS$_2$ flakes around the interaction region, the sudden drop in transmission was observed to confirm the successful optical evanescent-field deposition.

3. Q-Switched All-Fiber Laser

The schematic diagram of the Q-switched fiber laser combined with the fabricated WS$_2$ SA is demonstrated in Fig. 2. The ring cavity consists of a gain fiber, a wavelength division multiplexer (WDM), an optical coupler (OC), a polarization controller (PC), and a polarization independent isolator (ISO), along with fabricated saturable absorber. A 1 m long erbium doped fiber (EDF) (Er80-8/125) was employed as the gain medium. The EDF was pumped by a 976 nm laser diode (LD). The PC was engaged to achieve different polarization orientation states. The PI-ISO was used to force the unidirectional operation in the fiber ring cavity and the 10% portion of the laser was coupled out from the cavity via the optical coupler. The total length of the fiber laser cavity was about 9 m. Temporal and spectral profiles of the Q-switched fiber laser output are recorded by a fast electro-photonic detector followed by a digital oscilloscope (Tektronix TDS 784D) and an optical spectrum analyzer (Yokogawa AQ6370 B).

The laser started the continuous-wave lasing at the pump power of ~200 mW, and the Q-switched operation obtained at 295 mW. The threshold of the fiber laser was relatively high due to the primarily large intra-cavity loss induced by the WS$_2$-deposited fiber taper SA which could be optimized by managing the ring cavity and sample preparation. The performance of fiber laser including optical spectrum and output pulses are depicted in Fig. 3. The 3-dB bandwidth of the optical spectrum is measured to be ~1 nm at the center wavelength of 1565 nm as shown in Fig. 3(a). The pulse trains of laser in different pump power are illustrated in Fig. 3(b), which prove the robust operation of Q-switching pulses. In contrast to mode-locking operation which is repetition rate corresponding to the cavity length, the repetition rate of the Q-switched pulses can be varied with reference to pump power. When the pump power was increased, the repetition rates of output stable pulse trains simultaneously increased and the pulse duration monotonically decreases, which are the typical features of passively Q-switched lasers. Fig. 3(c) shows the repetition rates and pulse duration versus incident pump powers. The repetition rate increased from 33 kHz to 108 kHz while the pump power increasing from 295 mW to 603 mW, and the pulse widths decreased from 3 μs to 1.3 μs.

When the pump power was over 600 mW, the Q-switched pulses became unstable. The possible reason for the unstable Q-switching could be the over-saturation of the SA at higher pump intensity, which has been reported this kind of unstable phenomenon [25], [26]. However, after the pump power was decreased from 600 mW, the stable Q-switched operation was observed again with the same characteristics. This phenomenon indicated that the WS$_2$-deposited fiber
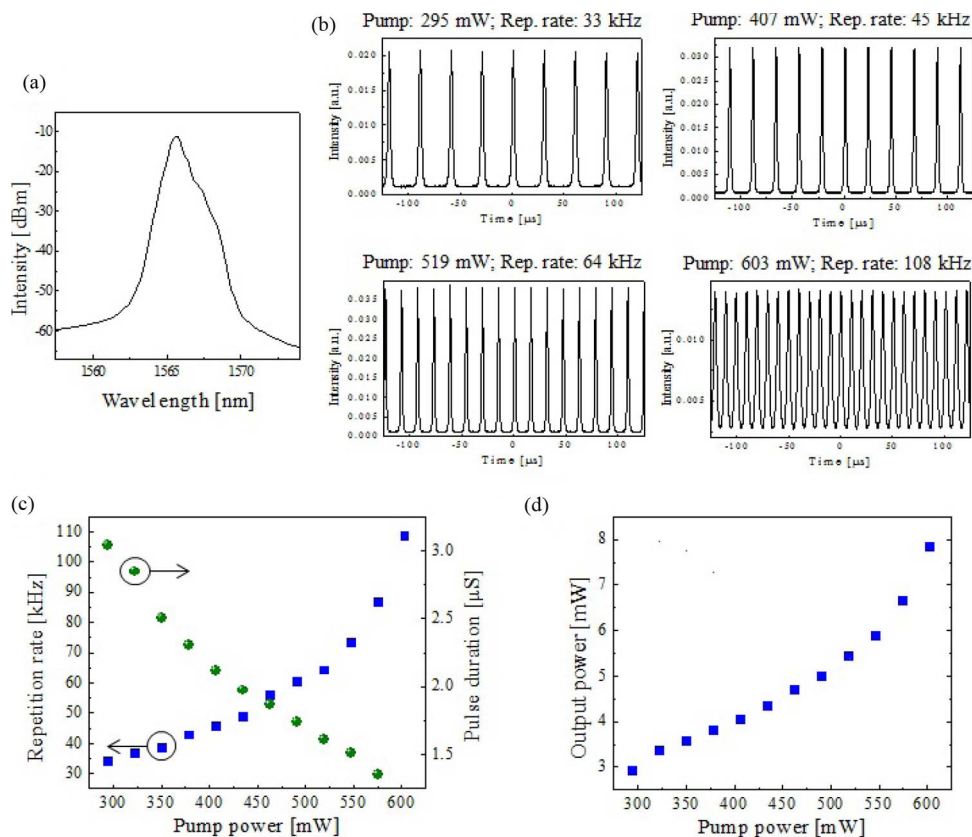
Fig. 3. Q-switched operation. (a) Optical spectrum. (b) Q-switched pulse trains with different pump powers. (c) Repetition rates and pulse duration versus incident pump powers. (d) Average output power versus incident pump power.

taper SA was not destroyed by the thermal accumulation and that there was no thermal damage in SA even at maximum pump power of LD (750 mW). Moreover, the Q-switched output pulses were stable and robust at the entire different repetition rate and pump power.

The shortest pulse duration of 1.3 μs was similar to the reported passively Q-switched fiber lasers based on graphene and CNT SAs [25], [26]. The pulse duration can be improved by shortening the laser cavity and optimization of saturable absorber fabrication process. The average output power and pulse energy versus incident pump power were depicted in Fig. 3(d). At the pump power of 603 mW, the maximum average output power was 7.84 mW, which is comparable with some other reported Q-switched fiber lasers. Even though the pulse energy is not that much high in comparison with the laser using conventional semiconductor-based SAs, further improvement of pulse energy is possible by optimizing the fiber taper SA fabrication as well as increasing the output ratio of the tap coupler in the ring cavity which we only used 10%.

Finally, we confirmed the functionality of WS_2-deposited fiber taper SA by inserting a non-deposited fiber taper into the same laser cavity and no pulse generation was observed. It confirms that the Q-switched pulses originate from the WS_2 materials not the bare fiber taper. The Q-switching results confirmed the pulse shaping ability of the WS_2 which is comparable with previously reported carbon materials. However, in the case of WS_2, there were no hazardous materials in the preparation process, unlike dichlorobenzene in CNT or additional polymer and composite, which cause a decrease in the damage threshold. We also need to consider that the WS_2 [27]–[30] is a new emerging nanomaterial in this field of study like $MoSe_2$ [31] and black phosphorous [32] and that their nonlinear optical properties should be studied in more detail for better comparison between these new materials and carbon materials like CNT and graphene.

4. Conclusion

In summary, we demonstrate the application of WS_2-deposited fiber taper, which can be employed as Q-switcher in a fiber ring cavity, for the first time to the best of our knowledge, to generate Q-switched short pulses. The advantages of the proposed WS_2 SA include all-fiber configuration, long nonlinear interaction length, flexibility, high optical damage threshold, and polymer free material. The SA fabrication process is based on the evanescent field interaction of a fiber taper with few-layer WS_2 flakes. Moreover, the deposition process can be controlled by continues in situ monitoring of the fiber taper transmission. We have successfully obtained an all-fiber passively Q-switched Erbium-doped fiber laser, including the WS_2-deposited fiber taper. The results indicate that the WS_2 has comparable optical property in a Q-switched fiber laser, and both the repetition rate and the output power could be tuned and increased significantly.

References

[1] S. Adachi and Y. Koyamada, "Analysis and design of Q-switched erbium-doped fiber lasers and their application to OTDR," *J. Lightw. Technol.*, vol. 20, no. 8, pp. 1506–1511, Aug. 2002.

[2] A. S. Kurkov, "Q-switched all-fiber lasers with saturable absorbers," *Laser Phys. Lett.*, vol. 8, no. 5, pp. 335–342, May 2011.

[3] N. Sarukura, Y. Ishida, H. Nakano, and Y. Yamamoto, "CW passive mode locking of a Ti:Sapphire laser," *Appl. Phys. Lett.*, vol. 56, no. 9, p. 814, Dec. 1990.

[4] B. Braun, F. X. Kärtner, U. Keller, J. P. Meyn, and G. Huber, "Passively Q-switched 180-ps Nd:LaSc3(BO3)4 microchip laser," *Opt. Lett.*, vol. 21, no. 6, pp. 405–407, Mar. 1996.

[5] F. Shohda, T. Shirato, M. Nakazawa, K. Komatsu, and T. Kaino, "A passively mode-locked femtosecond soliton fiber laser at 1.5 μm with a CNT-doped polycarbonate saturable absorber," *Opt. Exp.*, vol. 16, no. 26, pp. 21191–21198, Dec. 2008.

[6] Q. Bao *et al.,* "Atomic-layer graphene as a saturable absorber for ultrafast pulsed lasers," *Adv. Funct. Mater.*, vol. 19, no. 19, pp. 3077–3083, Oct. 2009.

[7] G. Sobon, J. Sotor, and K. M. Abramski, "Passive harmonic mode-locking in Er-doped fiber laser based on graphene saturable absorber with repetition rates scalable to 2.22 GHz," *Appl. Phys. Lett.*, vol. 100, Apr. 2012, Art. ID. 161109.

[8] U. Keller *et al.,* "Semiconductor Saturable Absorber Mirrors (SESAM's) for femtosecond to nanosecond pulse generation in solid-state laser," *IEEE J. Sel. Topics Quantum Electron.*, vol. 2, no. 3, pp. 435–453, Sep. 1996.

[9] S. Yamashita *et al.,* "Saturable absorbers incorporating carbon nanotubes directly synthesized onto substrates and fibers and their application to mode-locked fiber lasers," *Opt. Lett.*, vol. 29, no. 14, pp. 1581–1583, Jul. 2004.

[10] K. Wang *et al.,* "Ultrafast saturable absorption of two-dimensional MoS_2 nanosheets," *ACS Nano*, vol. 7, no. 10, pp. 9260–9267, Oct. 2013.

[11] B. Radisavljevic, A. Radenovic, J. Brivio, V. Giacometti, and A. Kis, "Single-layer MoS_2 transistors," *Nature Nanotechnol.*, vol. 6, no. 3, pp. 147–150, Feb. 2011.

[12] K. F. Mak, C. Lee, J. Hone, J. Shan, and T. F. Heinz, "Atomically thin MoS_2: A new direct-gap semiconductor," *Phys. Rev. Lett.*, vol. 105, no. 13, Sep. 2010, Art. ID. 136805.

[13] J. Du *et al.,* "Ytterbium-doped fiber laser passively mode locked by few-layer Molybdenum Disulfide (MoS_2) saturable absorber functioned with evanescent field interaction," *Sci. Rep.*, vol. 4, Sep. 2014, Art. ID. 6346.

[14] R. Khazaeinezhad, S. H. Kassani, H. Jeong, D.-I. Yeom, and K. Oh, "Mode-locking of Er-doped fiber laser using a multilayer MoS_2 thin film as a saturable absorber in both anomalous and normal dispersion regimes," *Opt. Exp.*, vol. 22, no. 19, pp. 23732–23742, Sep. 2014.

[15] D. Mao *et al.,* "WS_2 mode-locked ultrafast fiber laser," *Sci. Rep.*, vol. 5, no. 7965, pp. 1–7, Jan. 2015.

[16] R. Khazaeinezhad, S. H. Kassani, H. Jeong, D.-I. Yeom, and K. Oh, "Femtosecond soliton pulse generation using evanescent field interaction through Tungsten disulfide (WS_2) film," *J. Lightw. Technol.*, vol. 33, no. 17, pp. 3550–3557, Sep. 2015.

[17] R. I. Woodward *et al.,* "Tunable Q-switched fiber laser based on saturable edge-state absorption in few-layer molybdenum disulfide (MoS_2)," *Opt. Exp.*, vol. 22, no. 25, pp. 31113–31122, Dec. 2014.

[18] R. Khazaeinezhad *et al.,* "Ultrafast pulsed all-fiber laser based on tapered fiber enclosed by few-layer WS_2 nanosheets," *IEEE Photon. Technol. Lett.*, vol. 27, no. 15, pp. 1581–1584, Aug. 2015.

[19] P. Yan *et al., "Microfiber-based WS_2-film saturable absorber for ultra-fast photonics,"* *Opt. Mater. Exp.*, vol. 5, no. 3, pp. 479–489, Feb. 2015.

[20] R. Khazaeinezhad *et al.,* "Saturable optical absorption in MoS_2 nano-sheet optically deposited on the optical fiber facet," *Opt. Commun.*, vol. 335, pp. 224–230, Jan. 2015.

[21] S. M. Tseng and C. L. Chen, "Side-polished fibers," *Appl. Opt.*, vol. 31, no. 18, pp.3438–3447, Jun. 1992.

[22] T. A. Birks and Y. W. Li, "The shape of fiber tapers," *J. Lightw. Technol.*, vol. 10, no. 4, pp. 432–438, Apr. 1992.

[23] J. N. Coleman *et al.,* "Two-dimensional nanosheet produced by liquid exfoliation," *Science*, vol. 331, no. 6017, pp. 568–571, Feb. 2011.

[24] D. B. Velusamy *et al.* "Flexible transition metal dichalcogenide nanosheets for band-selective photodetection," *Nat. Commun.*, vol. 6, no. 8063, Sep. 2015.

[25] D. P. Zhou, L. Wei, B. Dong, and W. K. Liu, "Tunable passively Q-switched erbium-doped fiber laser with carbon nanotubes as a saturable absorber," *IEEE Photon. Technol. Lett.*, vol. 22, no. 1, pp. 9–11, Jan. 2010.

[26] J. Liu, S. Wu, Q. H. Yang, and P. Wang, "Stable nanosecond pulse generation from a graphene-based passively Q-switched Yb-doped fiber laser," *Opt. Lett.*, vol. 36, no. 20, pp. 4008–4010, Oct. 2011.

[27] R. Khazaeinezhad *et al.,* "Optical deposition of MoS_2 on an optical fiber facet, its reflectometry and nonlinear response," in *Proc. IEEE Photon. Conf.*, Sep. 2013, pp. 265–266.

[28] R. Khazaeinezhad *et al.,* "Mode-locked all-fiber lasers at both anomalous and normal dispersion regimes based on spin-coated MoS_2 nano-sheets on a side-polished fiber," *IEEE Photon. J.*, vol. 7, no. 1, Feb. 2015, Art. ID. 1500109.

[29] S. H. Kassani *et al.,* "All-fiber Er-doped Q-Switched laser based on Tungsten Disulfide saturable absorber," *Opt. Mater. Exp.*, vol. 5, no. 2, pp. 373–379, Jan. 2015.

[30] R. Khazaeinezhad, S. H. Kassani, H. Jeong, D.-I. Yeom, and K. Oh, "Passively Mode-locked Fiber Laser based on CVD WS2," in *Proc. IEEE Cleo*, May 2015, pp. 1–2.

[31] R. I. Woodward *et al.,* "Wideband saturable absorption in few-layer molybdenum diselenide (MoS_2) for Q-switching Yb-, Er- and Tm-doped fiber lasers," *Opt. Exp.*, vol. 23, no. 15, pp. 20051–20061, Jun. 2015.

[32] Y. Chen *et al.,* "Mechanically exfoliated black phosphorus as a new saturable absorber for both Q-switching and Mode-locking laser operation," *Opt. Exp.*, vol. 23, no. 10, pp. 12823–12833, May 2015.